ELSEVIER

Applied Energy **48** (1994) 335–351

0306-2619/94/$7.00

Forced Steady-State Convections from Pin-Fin Arrays

M. A. Tahat, R. F. Babus'Haq & S. D. Probert

Department of Applied Energy, Cranfield University, Bedford, UK, MK43 0AL.

ABSTRACT

The steady-state thermal and air-flow resistance performances of horizontally-based pin-fin assemblies have been investigated experimentally. The effects of varying the geometrical configurations of the pin-fins and the air-flow rates have been studied. The optimal pin-fin separation $S_{x_{opt}}$ *in the span-wise direction, to achieve a maximum rate of heat transfer from the assembly, is* $1{\cdot}0 \pm 0{\cdot}2\ mm \leq S_x \leq 3{\cdot}0 \pm 0{\cdot}2\ mm$ *for the pin-fins arranged either in the in-line or the staggered array. The optimal pin-fin separations in the stream-wise direction for these two arrays are* $7{\cdot}6 \pm 0{\cdot}2$ *mm and* $7{\cdot}8 \pm 0{\cdot}2$ *mm respectively. The general correlation of the data is:*

$$Nu = 0{\cdot}355 \left(\frac{S_x}{X}\right)^{0{\cdot}0446} \left(\frac{S_y}{L}\right)^{0{\cdot}048} Re^{0{\cdot}585}$$

NOTATION

A	Area(m^2)
C_p	Specific heat at atmospheric pressure (J/kgK)
d	Diameter of each pin-fin (see Fig. 1) (m)
f	Friction factor
F	Shape factor
G	Mass flow rate per unit area (kg/m^2s)
h	Heat transfer coefficient (W/m^2K)
H	Vertical protrusion upwards of each pin-fin (see Fig. 1) (m)
k	Thermal conductivity (W/mK)
L	Length of the pin-fin assembly's horizontal base (see Fig. 1) (m)
$\dot{m}$	Mass flow rate (kg/s)
N	Number of pin-fins in the heat exchanger
Nu	Nusselt number of the forced air-flow (as defined in eqn (13))

p_p Air pressure (N/m^2)
Q Steady-state rate of heat transfer (W)
Re Reynolds number of the forced air-flow (as defined in eqn (9))
S Separation between adjacent pin-fins (see Fig. 2) (m)
T Steady-state temperature (K)
V Mean inlet velocity (m/s)
W Span-wise width of the wind-tunnel (see Fig. 1) (m)
X Span-wise width of the pin-fin assembly's horizontal base (see Fig. 1) (m)

μ Dynamic viscosity of the air at temperature T_{av} (kg/ms)
ρ Density of the air at temperature T_{av} (k/m^3)
σ Stefan–Boltzmann constant (W/m^2K^4)

Subscripts

a Air
av Average
b Base of the pin-fin array
ff Free unobstructed flow
in Inlet
max Maximum
opt Optimal
out outlet
s Surface
x Span-wise direction
y Stream-wise direction

THE PROBLEM

As power levels and chip densities of electronic equipment increase, the design engineer is faced with selecting the optimal heat sink (e.g. extruded plate fins, or cast circular or square pin-fins) which will dissipate reliably the required thermal power, subject to the space and air-flow restraints.[1] This is necessary to limit the temperatures of the electronic components to be less than 65°C in order to ensure a sufficiently long mean time between failures.

Fins are used primarily to increase the area and consequently to enhance the heat-transfer rate from a body, and hence are at a lower temperature than the base-plate.[2] In designing the cooling configuration for a turbine blade, circular pin-fins at the trailing-edge region may also serve a structural purpose by holding the suction and pressure surfaces of

the blade together. They span the distance between the suction and pressure surfaces which form the endwalls of the cooling passage.[3,4]

In general, the heat transfer from a pin-fin assembly to the surrounding environment occurs by convection and radiation through the air. The rate of heat transmission depends on: (i) the temperature distributions over the pin-fins as well as the assembly's base; (ii) the pin-fin geometry; (iii) the air flow rate; and (iv) for low air-flow rates, the orientation of the heat exchanger.

For a constant temperature of the base plate of the pin-fin assembly, the heat transmission can be enhanced only by increasing the mean heat-transfer coefficient, the surface area or both. An increase in the heat-transfer coefficient can be achieved via forced (rather than free) convection (i.e. employing a fan) or changing the geometrical configuration of the heat exchanger. However, in practice, this means is limited by the maximum air pressure-drop through the assembly, which in itself is dictated by the maximum electrical power of the fan. However, an extended surface area can be achieved via introducing more pin-fins.

The design criteria of fins are different for various applications, but the primary concerns are to limit the weight, the volume and cost of the assembly as well as optimise the running cost of the heat exchanger. Therefore, it is highly desirable to optimise the size and the configuration of the fins for each energy running cost.[5] The optimal dimensions can be those for which the maximum rate of heat is dissipated either for a given weight or arrangement of the fin arrays or mean air-flow speed. The effects of pin-fin spacing, in both the stream-wise and span-wise directions, on the steady-state rate of heat transfer have been investigated experimentally for different air-flow rates. The pin-fins were arranged either in the in-line or the staggered configuration (see Fig. 2, later).

EXPERIMENTAL HEAT-TRANSFER RIG

Pin-fin assembly

The array consisted of circular-section pin-fins (d = 6·35 mm and H = 60 mm) protruding vertically upwards from a 300 mm × 170 mm horizontal rectangular base (see Fig. 1). The number of fins can be varied in accordance with the fin spacing. For the smallest pin-fin spacing, the maximum number of pin fins is 629, whereas for the largest spacing, the array consists of only 12 pin-fins. The spacing can be varied from 3·2 to 69·6 mm in the span-wise direction and from 1·0 to 81·6 mm in the stream-wise direction (see Fig. 2). The pin-fins can be easily removed and

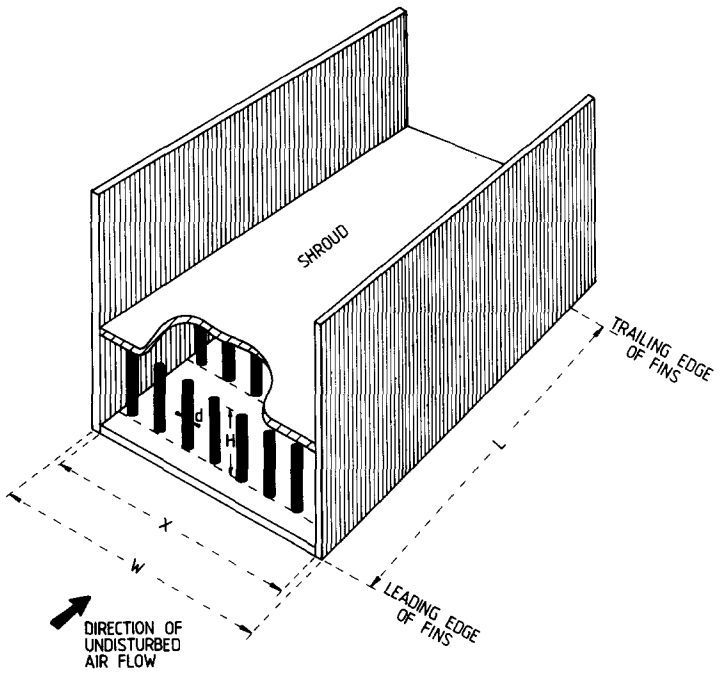

Fig. 1. Schematic representation of the shrouded aligned pin-fin assembly.

replaced with studs made from the same material as the assembly base: when screwed in, their heads are flush with the upper surface of the horizontal base plate. The rectangular base as well as the pin-fins were manufactured from a light aluminum alloy (i.e. duralumin). For each test, the pin-fin height was kept constant with zero clearance between the tips of the pin-fins and the shroud (i.e. in full contact with the shroud).

Heating system

The base of the exchanger was heated almost uniformly by four electric-resistor strips, each rated at 500 W: this was the main heater. The assembly was firmly bolted together at the bottom surface of the rectangular base (see Fig. 3). The presence of thin layers of high thermal-conductivity heat-sink putty ensured that good thermal contacts existed between the main heater and the rectangular base, as well as between the fin roots and the rectangular base.

The lower horizontal surface and sides of the main heater block (when operational) were insulated thermally with 80-mm thick mineral-wool blankets. A horizontal guard heater, rated at 500 W, was positioned, parallel to the main heater, below the mineral-wool blanket, with yet another 80-mm layer of mineral-wool placed below it (see Fig. 3). The

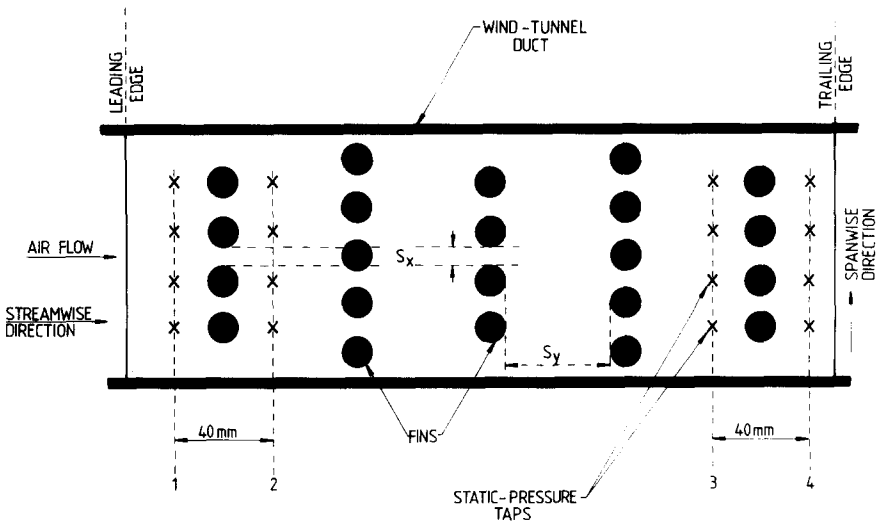

Fig. 2. Schematic horizontal-section representation of the locations of the staggered array of pin-fins and the static-pressure taps.

whole system of heat-exchanger base, heaters and guard heater, with associated thermal insulation, was located in, and protected by, a well-fitting open-topped wooden box. The horizontal upper edges of this box and the top surfaces of the laterally-placed thermal insulant, during each experiment, were flush with the upper surface of the multi-component rectangular base, from which the fins protruded upwards.

The power supplied to the main heater could be adjusted by altering the variac setting and was measured by an in-line electronic Wattmeter. The dissipation in the guard heater was adjusted until the steady-state temperature difference across the layer of insulant, sandwiched between the heaters, was zero. Then, under all the test conditions employed, more than 98% of the heat generated in the main heater passed to the air of the surrounding environment, through the finned heat exchanger. The steady-state temperatures at the base of the fin array were measured by an appropriately distributed set of six copper–constantan thermojunctions, embedded within the rectangular base. Each thermojunction was bonded in position with a thin layer of epoxy resin, so as to ensure good thermal contact ensued. The average value obtained from these appropriately-located thermojunctions was regarded as the mean overall base temperature. This was maintained constant during each experiment at $40 \pm 0{\cdot}5°C$.

The inlet and the outlet air-stream temperatures in the wind-tunnel duct were measured using eight thermocouples: four were located immediately prior to the entrance of the pin-fin assembly and another four

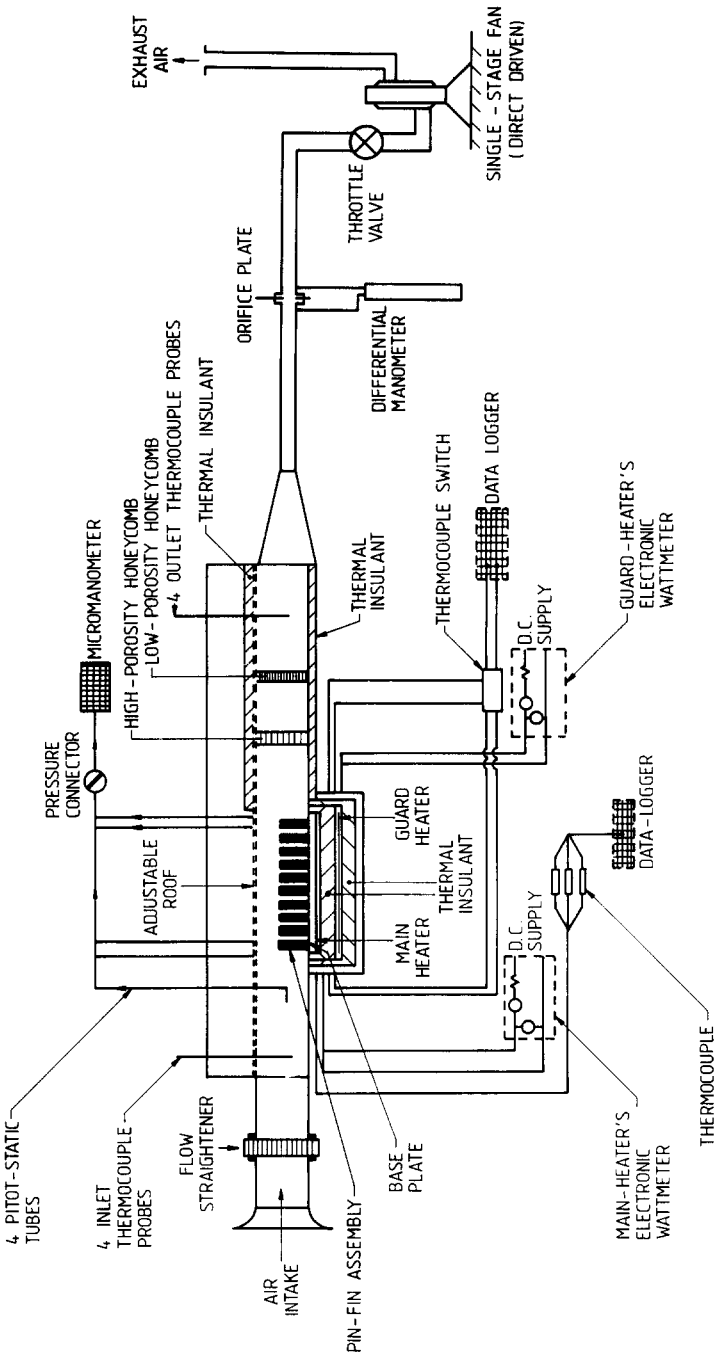

Fig. 3. Schematic representation of the experimental rig and associated instruments.

downstream of the array. These could be traversed across the whole inlet and outlet cross-sections of the wind-tunnel duct (see Fig. 3). All the thermocouples, as well as those indicating the ambient air temperature were connected, through ribbon cables, to a data-logger which was used to interpret the temperatures, each half hour, until steady-state conditions were attained.

Wind tunnel

The main body of the rectangular cross-sectioned wind-tunnel duct (see Fig. 3) was manufactured from wood and was 2 m long with a constant internal width of 240 mm. However, the uniform vertical height of the duct, and hence the duct's cross-sectional area, could be varied. Different duct heights were obtained by means of an adjustable horizontal roof (or shroud). Approximately half-way along the length of the wind-tunnel duct was the test section. The roof and side walls of this test section were made of 6·35-mm thick Perspex, so enabling the fin array (and the air via smoke-flow visualisation around it) to be observed.

A bell-mouth section was fitted at the entrance of the wind tunnel duct, followed by a resin-impregnated, low porosity, cardboard honeycomb flow-straightener. The exhaust air from the pin-fin assembly was passed through an insulated chamber, where mixing was accomplished by two resin-impregnated cardboard honeycombs, one being of relatively low porosity and the other of higher porosity. The latter was situated upstream of the former. The two honeycombs were mounted perpendicular to the undisturbed flow-stream. At the exhaust end of the duct, a gradual area-contraction section was attached. It was connected, via a plastic pipe, to a single-speed, single-stage fan, which was capable of providing a maximum flow rate of 0·242 kg/s, and preceded by a throttle control valve. A differential manometer was employed to measure the pressure drop across an orifice plate, which had been calibrated according to BS 1042 (see Fig. 3), to indicate air-flow speeds.

The wind tunnel was operated in the suction mode, i.e. the fan sucked atmospheric air through the fin assembly and the test section via the bell-mouthed entrance section, with the fan and motor assembly on the exhaust side of the system. This avoided the air-stream being heated by the motor prior to its passage through the heat-exchanger assembly: this would thereby have reduced the cooling capability of the air.

The overall pressure drop along the heat exchanger was obtained via four sets of four static-pressure tappings located in the roof of the test section, i.e in a plane orthogonal to the direction of the mean air-flow (see Fig. 2). The velocity profile of the inlet air-stream to the fin assembly

was identified via four standard pitot-static tubes. A precision electronic analogue micromanometer was employed to measure the pressure drops.

HEAT TRANSMISSION

The prime objective of a heat exchanger is to transfer the maximum amount of energy per unit temperature-difference applied across it. Thus, the steady-state rate of heat transfer from the pin-fin arrays is

$$\dot{Q}_{\text{total}} = \dot{Q}_{\text{convection}} + \dot{Q}_{\text{radiation}} + \dot{Q}_{\text{losses}} \tag{1}$$

for a constant ΔT (= $T_{\text{out}} - T_{\text{in}}$), where

$$\dot{Q}_{\text{convection}} = \dot{m} C_{p,a} \, \Delta T \tag{2}$$

The specific heat of still air at atmospheric pressure[6] is

$$C_{p,a} = \left[9{\cdot}82 + 8 \times 10^{-4} \left(\frac{T_{\text{out}} + T_{\text{in}}}{2}\right)\right] \times 10^2 \tag{3}$$

for 250 K $\leq (T_{\text{out}} + T_{\text{in}})/2 \leq$ 400 K.

The steady-state rate of convection from the heat exchanger can also be represented by:

$$\dot{Q}_{\text{convection}} = h_{av} A_s \left[T_b - \left(\frac{T_{\text{out}} + T_{\text{in}}}{2}\right)\right] \tag{4}$$

where

$$A_s = XL + \pi DHN_x N_y \tag{5}$$

From eqns (2) and (4), the average convective heat-transfer coefficient

$$h_{av} = \frac{\dot{m} C_{p,a} \, \Delta T}{A_s \left[T_b - \left(\frac{T_{\text{out}} + T_{\text{in}}}{2}\right)\right]} \tag{6}$$

The steady-state rate of radiative heat transfer from pin-fin arrays is dependent on: (i) the temperatures of the radiating surfaces; (ii) the temperature distribution in the surrounding environment; (iii) the emissivities of the pin-fin and the base-plate surfaces (for example, due to their surface roughnesses) as well as the effective emissivity of the environment; (iv) the shielding effect of adjacent pin-fins. Hence, the temperatures of the radiating surfaces and the shielding effects will dictate the shape factor of the grey body.

The total steady-state rate of radiative heat transfer can be evaluated from

$$\dot{Q}_{\text{radiation}} = FA_s\sigma(T_b^4 - T_a^4) \tag{7}$$

However, under the considered conditions of the current investigation, the steady-state rate of radiative heat losses from the pin-fin assembly with polished surfaces (at near room temperatures) as well as the stray heat losses represented only ≤ 5% of the total steady-state rate of heat transfer. (In practice, rougher surfaces would lead to higher rates of radiative heat transfers but thicker boundary layers and so lower convective transfers. In addition, the increased roughness would contribute to the air flow resistance. Thus, an optimal roughness corresponding to the maximum rate of heat transfer would occur for each geometric and temperature distribution condition.) Therefore, for the present approximation, eqn (1) becomes

$$\dot{Q}_{\text{total}} \approx \dot{Q}_{\text{convection}} \tag{8}$$

Also, the Reynolds number (Re) is defined as

$$Re = \frac{G_{\max}d}{\mu_a} \tag{9}$$

where

$$G_{\max} = \frac{\dot{m}}{A_{\text{ff}}} \tag{10}$$

The dynamic viscosity of still air[6] is

$$\mu_a = \left[5 + 4{\cdot}5 \times 10^{-2}\left(\frac{T_{\text{out}} + T_{\text{in}}}{2}\right)\right] \times 10^{-6} \tag{11}$$

for 250 K ≤ $(T_{\text{out}} + T_{\text{in}})/2$ ≤ 400 K.

The free-flow sectional area of the pin-fin array, A_{ff}, is

$$A_{\text{ff}} = H(W - N_x d) \tag{12}$$

The Nusselt number (Nu) is defined as

$$Nu = \frac{h_{av}d}{k_a} \tag{13}$$

The thermal conductivity of still air[6] is

$$k_a = \left[3{\cdot}7 + 7{\cdot}5 \times 10^{-2}\left(\frac{T_{\text{out}} + T_{\text{in}}}{2}\right)\right] \times 10^{-3} \tag{14}$$

for 250 K ≤ $(T_{\text{out}} + T_{\text{in}})/2$ ≤ 400 K.

PRESSURE DROP

Often the specification of a heat exchanger will state the maximum pressure drop that can be accommodated in the system. In considering the current investigation, it was necessary to take into account the pressure drop at the entrance and the pressure rise at the exit that would occur due to flow-area changes. Losses that occur due to the flow through the pin-fins' assembly, i.e. frictional losses, were also considered. Pressure measurements via the static-pressure tappings, installed in the shroud along the pin-fin assembly (see Fig. 2), were recorded and the overall pressure drops were evaluated for all the conducted tests.

The overall pressure drop, Δp, across the heat exchanger is

$$\Delta p_{\text{overall}} = \Delta p_{1\to4} \tag{15}$$

The pressure loss due to flow through the pin-fin array is represented non-dimensionally by a friction factor, which is based on the D'Arcy relationship,[7] viz

$$f = \frac{2\,\Delta p_{2\to3}}{\left(\frac{L}{d}\right)\left(\frac{\dot{m}}{A_{\text{ff}}}\right)^2 \frac{1}{\rho}} \tag{16}$$

OBSERVATIONS

In-line configuration

For a constant configuration of the in-line pin-fin assembly and a fixed uniform spacing, S_y, of the pin-fins in the stream-wise direction, the steady-state rates of heat transfer were measured for several values of the uniform spacing, S_x, of the pin fins in the span-wise direction. By plotting the resulting heat loss per unit base area of the heat exchanger versus the pin-fin separations in the stream-wise direction (see Fig. 4), the optimal spacing in the span-wise direction was estimated to be in the range $1{\cdot}0 \pm 0{\cdot}2$ mm $< S_{x,\text{opt}} < 3{\cdot}0 \pm 0{\cdot}2$ mm, corresponding to the maximum rate of heat loss from the pin-fin assembly. Similar observations were made for the spacings in the stream-wise direction, where an optimal value of $\sim 7{\cdot}6 \pm 0{\cdot}2$ mm was established (see Fig. 5). Greater rates of heat dissipation from the pin-fin assembly were achieved at higher mean inlet velocities.

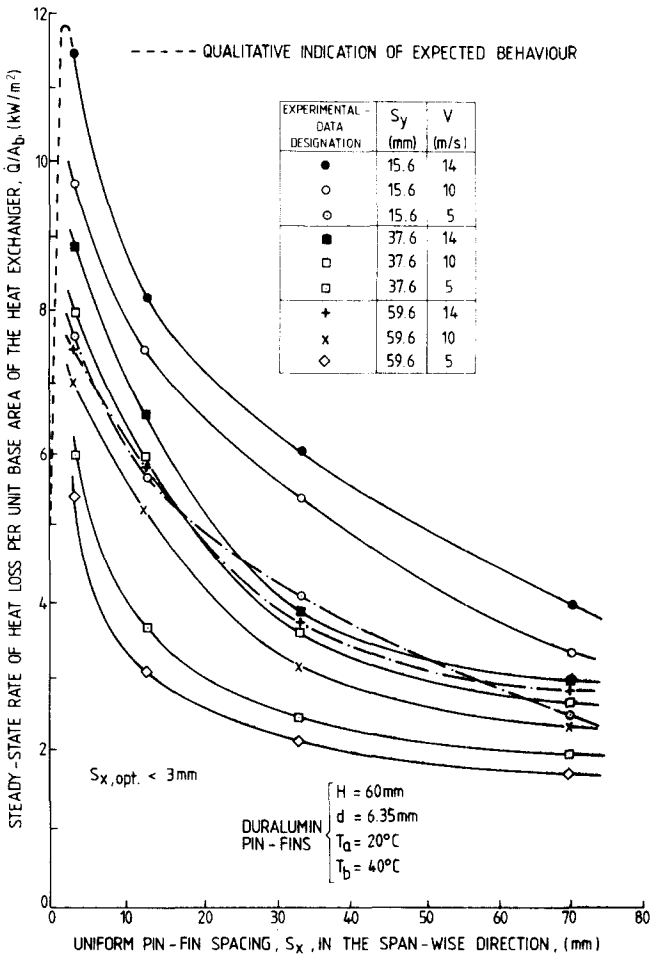

Fig. 4. Variation of the steady-state rate of heat loss with the pin-fin spacing in the span-wise direction for the in-line arrangement.

The results agree qualitatively with those of Jubran *et al.*[8] Their data were established with a heat-transfer rig based on the apparatus employed in this investigation. However their optimal spacings in the span-wise and the stream-wise directions were 2·5 times the diameter of the pin-fin, whereas, in the present set of measurements the ratio was only 0·3 and 1·2 respectively.

The effect of increasing the mean inlet velocity on the overall pressure drop is shown in Fig. 6: as the velocity increases, the pressure drop also increases. This is due to the flow contraction at the entrance of the heat exchanger and the flow expansion at its exit, as well as the frictional losses generated by the flow around the pin-fins. The effect of increasing

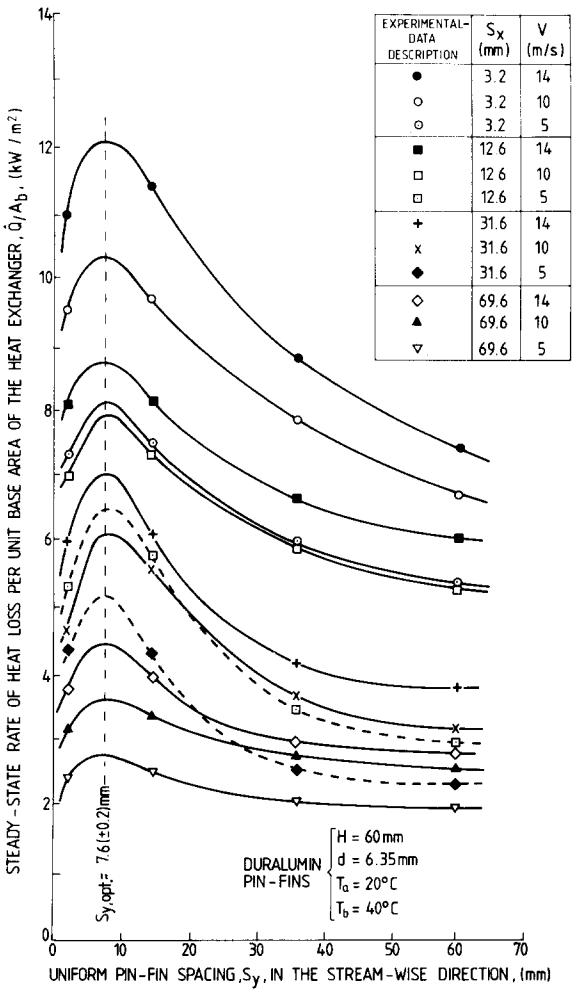

Fig. 5. As for Fig. 4, but with respect to the pin-fin spacing in the stream-wise direction for the in-line arrangement.

the pin-fin spacing in the span-wise and the stream-wise directions on the overall pressure drop is also shown in Fig. 6.

Staggered configuration

By adopting an analogous experimental procedure for testing the pin-fin assembly in the staggered configuration, the optimal spacing in the span-wise direction was similar to that when the pin-fins were in the in-line arrangement. However, an optimal value of 7·8 ± 0·2 mm was established in the stream-wise direction (see Figs 7 and 8). The overall pressure drop decreased, as expected, as both uniform pin-fin spacings were increased.

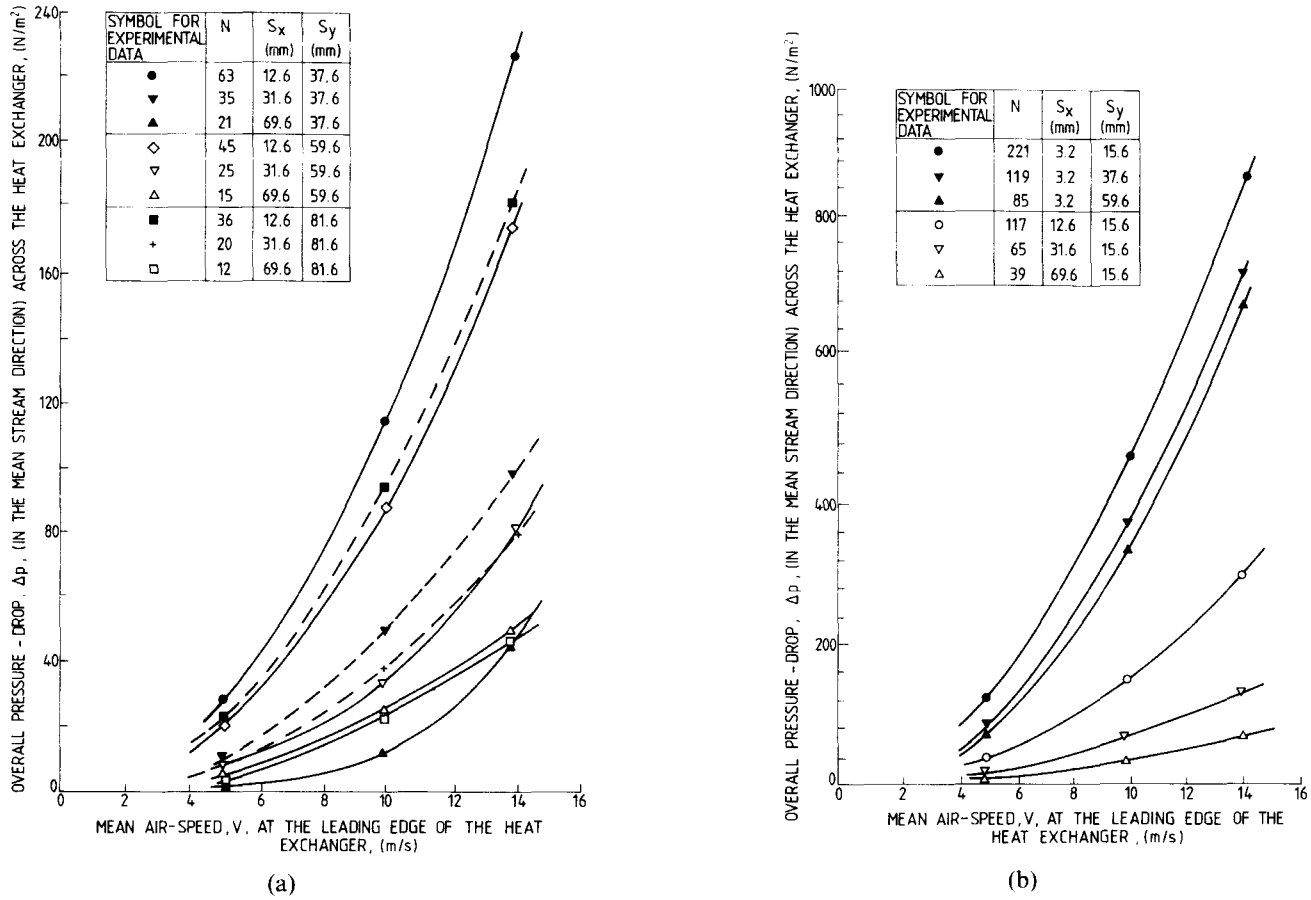

Fig. 6. Variations (see (a) and (b)), of the overall pressure drop with the mean inlet velocity for the in-line arrangement.

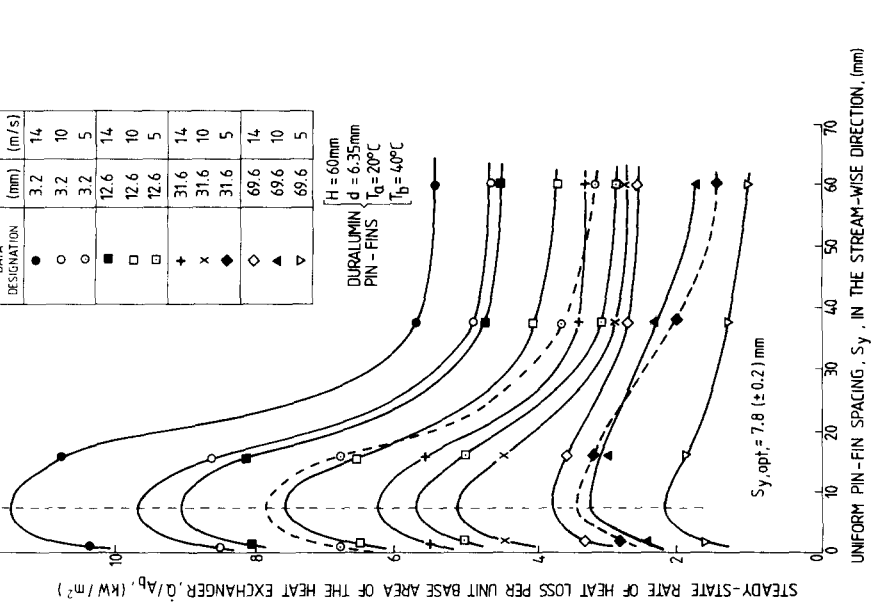

Fig. 8. As for Fig. 7, but with respect to the pin-fin spacing in the stream-wise direction for the staggered arrangement.

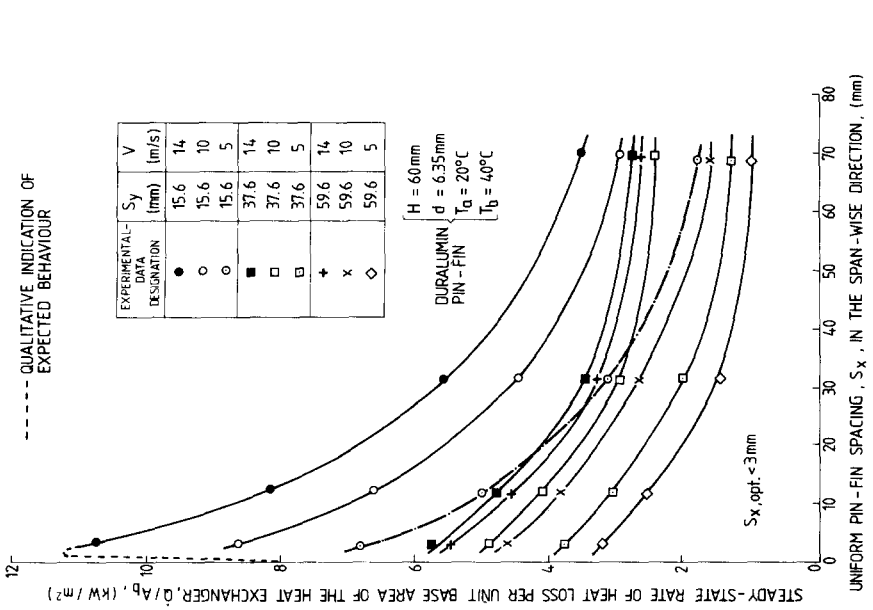

Fig. 7. Variation of the steady-state rate of heat loss with the pin-fin spacing in the span-wise direction for the staggered arrangement.

CORRELATION OF RESULTS

Several heat-transfer correlations for fin arrays have been deduced previously.[9,10] However, it is necessary to consider a form of correlation which would represent accurately the thermal characteristics of the pin-fin array. By incorporating the span-wise and the stream-wise spacings, a non-dimensional heat-transfer correlation of the following form was considered

$$Nu = f\left[\left(\frac{S_x}{X}\right), \left(\frac{S_y}{L}\right), Re\right] \tag{17}$$

To test the validity of eqn (17), a regression analysis was carried out. The dimensionless equation was expressed by

$$Nu = \alpha \left(\frac{S_x}{X}\right)^{\beta} \left(\frac{S_y}{Y}\right)^{\gamma} Re^{\delta} \tag{18}$$

where α, β, γ and δ are arbitrary constants, which are characteristic of the behaviour of the considered system. For the ranges of the experimental variables tested, a steady-state heat-transfer correlation was obtained by a least-squares fit, viz.

$$Nu = 0{\cdot}355 \left(\frac{S_x}{X}\right)^{0{\cdot}0446} \left(\frac{S_y}{L}\right)^{0{\cdot}048} Re^{0{\cdot}585} \tag{19}$$

for $1{\cdot}9 \times 10^3 \leq Re \leq 8{\cdot}9 \times 10^3$
$0{\cdot}019 \leq S_x/X \leq 0{\cdot}409$
$0{\cdot}003 \leq S_y/L \leq 0{\cdot}272$
$H = 60$ mm and $d = 6{\cdot}35$ mm

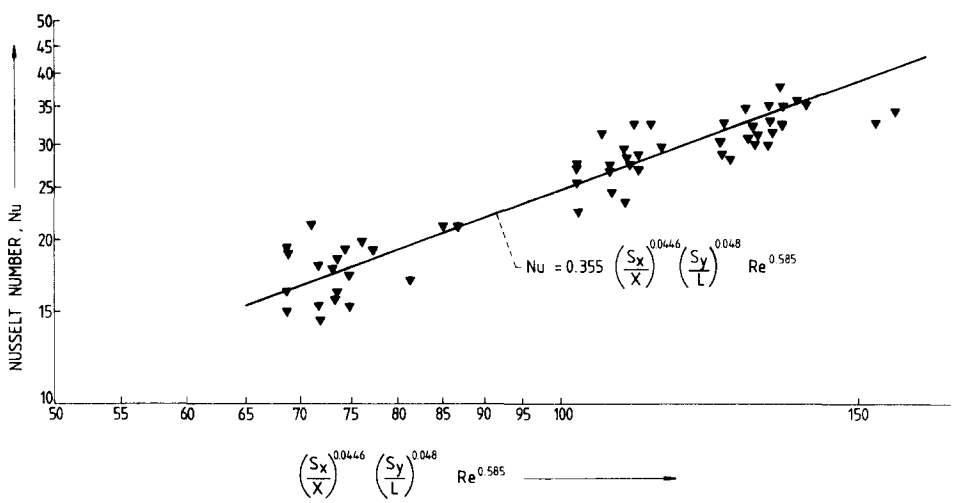

Fig. 9. Generalised heat-transfer correlation for pin-fin heat exchangers.

Equation (19) is illustrated in Fig. 9. It is evident that the Reynolds number can influence strongly the Nusselt number (i.e. the non-dimensional steady-state rate of heat transfer), whereas the ratios (S_x/X) and (S_y/L) can exhibit only small effects on the thermal performance of the pin-fin array. The deduced correlation agrees qualitatively with that of Jubran *et al.*[8]

CONCLUSIONS

The thermal performance of a shrouded vertical duralumin pin-fin assembly has been investigated experimentally. The optimal separation between the pin fins corresponding to the maximum rate of steady-state heat transfer from the assembly was deduced. In the span-wise direction, this was $S_x < 3{\cdot}0 \pm 0{\cdot}2$ mm for the in-line and the staggered configurations. Whereas, in the stream-wise direction, it was $\sim 7{\cdot}6 \pm 0{\cdot}2$ mm and $\sim 7{\cdot}8 \pm 0{\cdot}2$ mm for the in-line and staggered configurations respectively. A generalised heat-transfer correlation for pin-fin assemblies was established: it took the form

$$Nu = 0{\cdot}355 \left(\frac{S_x}{X}\right)^{0{\cdot}0446} \left(\frac{S_y}{L}\right)^{0{\cdot}048} Re^{0{\cdot}585} \tag{19}$$

REFERENCES

1. Doyle, A., Heat sink selection for high-power PGA packages, *Electron. Prod. Design*, **10**(10), 1989, 51–4.
2. Huang, L. J. & Shah, R. K., Assessment of calculating methods for efficiency of straight-fins of rectangular profile. *Int. J. Heat Fluid Flow*, **13**(3) (1992), 282–93.
3. VanFossen, G. J., Heat transfer coefficients for staggered arrays of short pin fins. *Trans. ASME, J. Engng Power*, **104**(2) (1982) 268–74.
4. Arora, S. C. & Abdel-Messeh, W., Characteristics of partial length circular pin fins as heat transfer augmentors for airfoil internal cooling passages. *Trans. ASME, J. Turbomachin.*, **112**(3) (1990) 559–65.
5. Chung, B. T. F. & Iyer, J. R., Optimum design of longitudinal rectangular fins and cylindrical spines with variable heat transfer coefficient, *Heat Transfer Engng.*, **14**(1) (1993) 31–42.
6. Incropera, F. P. & DeWitt, D. P., *Fundamentals of Heat and Mass Transfer*, 2nd edn, John Wiley, New York, 1985.
7. Jones, O. C., An improvement in the calculation of turbulent friction in rectangular ducts, *Trans. ASME, J. Fluid Engng.*, **98**(2) (1976) 173–81
8. Jubran, B. A., Hamdan, M. A. & Abdualh, R. M., Enhanced heat transfer, missing pin, and optimisation for cylindrical pin fin arrays. *Trans. ASME, J. Heat Transfer*, **115**(3) (1993) 576–83.

9. Metzger, D. E., Berry, R. A. & Bronson, J. P., Developing heat transfer in rectangular ducts with staggered arrays of short pin fins, *Trans. ASME, J. Heat Transfer*, **104**(4) (1982) 700–6.
10. Naik, S., Probert, S. D. & Shilston, M. J., Forced convection steady-state heat transfers from shrouded vertical-fin arrays, aligned parallel to an undisturbed air-stream. *Applied Energy*, **26**(2) (1987) 137–58.